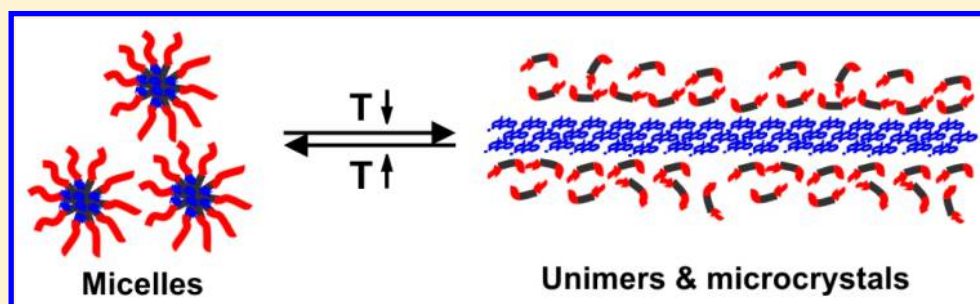


## Reversible Micro- and Nano- Phase Programming of Anthraquinone Thermochromism Using Blended Block Copolymers

Yumiao Zhang<sup>†,‡</sup> and Jonathan F. Lovell<sup>\*,†,‡</sup><sup>†</sup>Department of Biomedical Engineering and <sup>‡</sup>Department of Chemical and Biological Engineering, University at Buffalo, State University of New York, Buffalo, New York 14260, United States

## Supporting Information



**ABSTRACT:** Here, we present an approach to generate materials with programmable thermochromic transition temperatures (TTTs), based on the reversible microcrystallization of anthraquinone dyes with the assistance of blended Pluronic block copolymers. At temperatures above block copolymer critical micellization temperature (CMT), hydrophobic anthraquinone dyes, including Sudan blue II, were dispersed in copolymer micelles, whereas at lower temperature, the dyes formed microcrystals driven by dye–dye and dye–Pluronic molecular interactions. The crystallization process altered the optical properties of the dye with bathochromic shifts detectable by eye and the thermochromic process was fully reversible. Not only could Pluronic reversibly incorporate the anthraquinone dyes into micelles at elevated temperatures, but it also modulated the crystallization process and resulting morphology of microcrystals via tuning the molecular interactions when the temperature was lowered. Crystal melting transition points (and TTTs) were in agreement with the CMTs, demonstrating that the thermochromism was dependent on block copolymer micellization. Thermochromism could be readily programmed over a broad range of temperatures by changing the CMT by using different types and concentrations of Pluronics and combinations thereof.

## 1. INTRODUCTION

Stimuli responsive smart materials exist in nature<sup>1</sup> and have been extensively designed including photochromic,<sup>2,3</sup> halochromic,<sup>4,5</sup> piezochromic<sup>6,7</sup> and thermochromic<sup>8–11</sup> materials. Thermochromic materials, which alter color in response to changes in temperature, have gained attention,<sup>12–14</sup> varying from inorganic<sup>15</sup> to organic<sup>16</sup> and find a plethora of applications such as labels, sensors, toys, and space satellite coatings.<sup>17,18</sup> Usually the mechanism of organic thermochromism includes molecular species equilibrium, acid–base, stereoisomers, keto–enol tautomerism, lactim–lactam, or crystal structures.<sup>17</sup> Among these, polydiacetylenes with two different structures and phases,<sup>19–22</sup> some inorganic crystals,<sup>23</sup> organic crystals<sup>24</sup> and Schiff base materials<sup>25,26</sup> have attracted attention. To meet various practical applications, materials with customizable thermochromic transition temperatures (TTTs) are desired. However, such highly tunable materials have been difficult to design. Fabrication of nano and microcrystals has been studied to determine the intermediate states between the molecules and bulk crystals owing to their characteristic properties.<sup>27</sup> Nanostructured materials have been studied extensively and microcrystals are used in practical applications such as in semiconductors<sup>28</sup> and pharmaceuticals.<sup>29</sup> However, relatively

few studies have reported reversible transitions between micro and nano structured particles for thermochromism. In this work, we present a fully reversible thermochromic behavior with tunable TTTs based on micro and nano phase transformation of anthraquinone dyes in the presence of Pluronic block copolymers. At high temperature, hydrophobic anthraquinone dyes were dispersed in Pluronic micelles whereas at low temperature, the dyes formed microcrystals driven by the dye–dye and/or dye–Pluronic molecular interactions. The crystallization process altered the optical properties of the dye with a bathochromic change of color. Pluronic played a role in both solubilization of the hydrophobic dye and changing the crystallization process and morphology of microcrystals by molecular interactions. Nano and micro particle transition temperatures (or TTTs) were in accordance with the critical micellar temperature (CMT) of the Pluronic solution used as the stabilizer. Considering that CMTs can be modulated by different types of Pluronic, different concen-

Received: August 19, 2015

Revised: October 19, 2015

Published: December 1, 2015

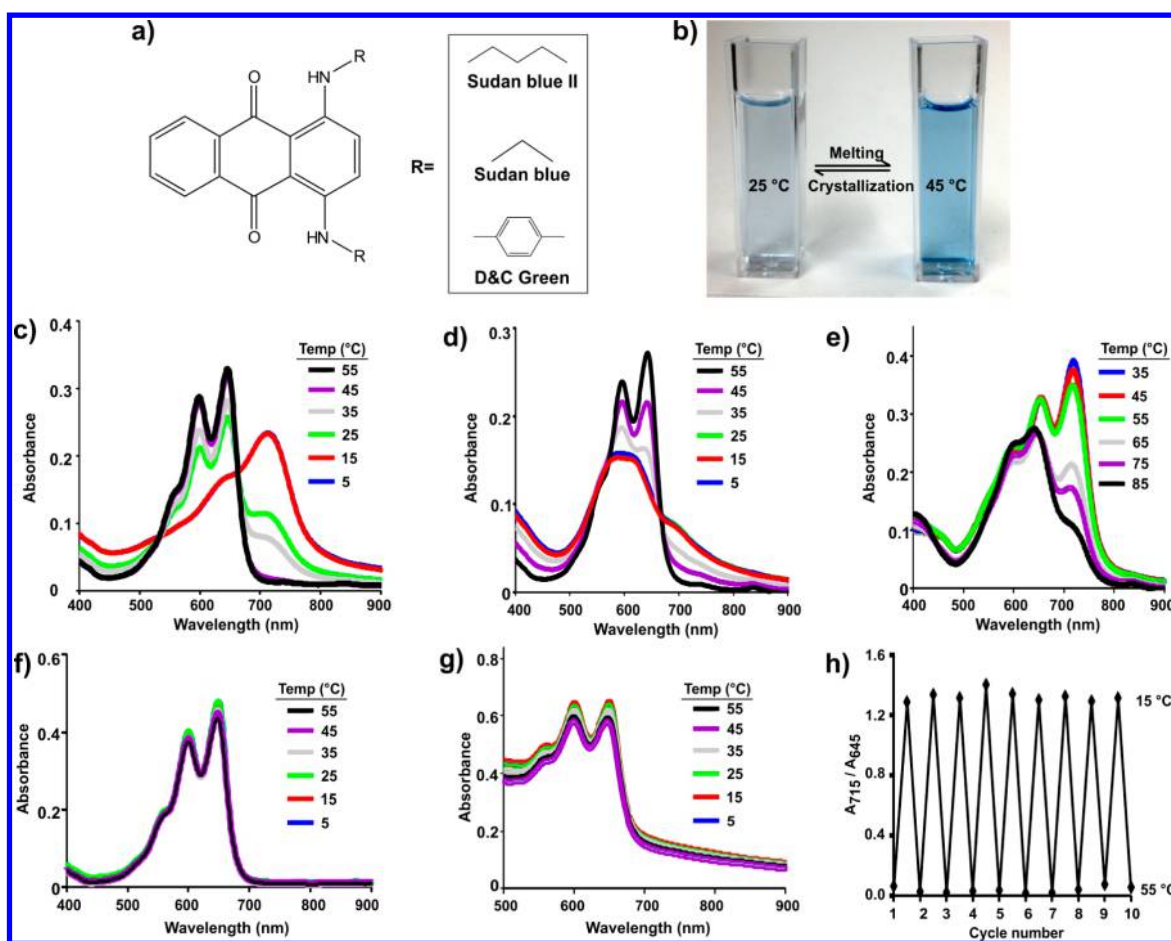


**Figure 1.** Reversible thermochromism of anthraquinones in the presence of Pluronic block copolymers. (a) Chemical structures of indicated anthraquinone dyes. (b) Photograph of  $2 \mu\text{M}$  Sudan blue II in 1% Pluronic F108 at indicated temperatures. Absorption of dyes in 1% Pluronic F108 at indicated temperatures for (c) Sudan blue II, (d) Sudan blue and (e) D&C green. Absorption of Sudan blue II at indicated temperatures in (f) 1% TX 100 or (g) DMPC liposomes. (h) Reversible thermochromism of Sudan blue II in 1% F108, as measured by the ratio of the absorbance at 715 to 645 nm, during thermal cycling between 55 and 15 °C.

trations of Pluronic, or blended Pluronic, TTTs could be accordingly broadly and precisely controlled.

## 2. EXPERIMENTAL SECTION

**2.1. Materials.** 1,4-Bis(butylamino)anthraquinone (Sudan blue II, Sigma #306436); 1,4-Bis(ethylamino)-9,10-anthraquinone (Sudan blue, Sigma #229121); D&C Green (Solvent Green 3, Spectrum #D1126). Pluronic F127 (Sigma, #P2443); Pluronic F108 (Sigma, #542342); Pluronic F68 (Sigma, #412325); Dimyristoylphosphatidylcholine (DMPC, Avanti #850345P); Triton X-100 (Sigma, #X100-500 ML); Tetrahydrofuran (THF, Avantor, #9440-03); *N,N*-Dimethylformamide (Fisher, D119-4); Chloroform (Fisher, #C298-4).

**2.2. Preparations of Microcrystals and Micelles.** Anthraquinone particles were prepared by a conventional reprecipitation method. Briefly, a stock solution of 10 mM 1,4-Bis(butylamino)-anthraquinone (Sudan Blue II), or 10 mM 1,4-Bis(ethylamino)-9,10-anthraquinone (Sudan blue), or 10 mM D&C Green in THF was prepared first. Then 200  $\mu\text{L}$  of the stock solution was injected into 10 mL of 10% (w/v) Pluronics (F127, F108 or F68) aqueous solution or into Triton X-100 surfactants aqueous solution 10% (w/v) for the control with vigorous stirring. After stirring for 3 min, the solution was maintained undisturbed for about 4 h to stabilize the structure. The resulting solutions were diluted (1 in 10) for absorbance measurements at different temperatures or subjected to spinning at 2000g for 5 min to harvest microcrystals from the pellet. Anthraquinone liposomes were prepared by dissolving 2 mg dye and 19.9 mg dimyristoylphos-

phatidylcholine (DMPC) in a small amount ( $\sim 500 \mu\text{L}$ ) of chloroform, and then the solvent was evaporated under a nitrogen stream. The resulting film was rehydrated in 1 mL distilled water and sonicated for 15 min, followed by filtering through a 0.2  $\mu\text{m}$  syringe filter. Crystallization at different temperatures was conducted by preparing dyes as described above, but in 1% F108. After adding THF stock solution and stirring for 3 min, solutions were kept at 4 °C, 25 °C, or other temperatures (37 °C or 45 °C in a programmable thermal controller by MJ Research) for 4 h. Microcrystals were then harvested following centrifugation at 2000g for 5 min, and scanning electron microscopy (SEM) was performed.

**2.3. Characterization.** Absorbance was measured with a Lambda 35 UV/vis spectrophotometer (PerkinElmer) coupled with a Peltier temperature controller (PerkinElmer, PTP-1 Peltier System). Samples were placed in the cuvette holder for at least 15 min for heat equilibration at varying temperatures. For the 15–55 °C thermal cycling experiment, at least 30 min were required to cool down the samples at each cooling cycle.

Field emission Scanning electron microscope (JEOL JSM-6500F) with an accelerating voltage of 5000 V was used to determine the morphology. Microparticles were harvested by centrifugation at 2000g for 5 min, and the pellet was washed by water 3 times before characterization.

Dynamic light scattering measurement was carried out using a Nano ZS90 Zetasizer (Malvern Instruments) after heating the sample to 70 °C for 30 min.

X-ray diffraction powder pattern was carried out on a Rigaku Ultima IV with operating conditions 40 kV, 44 mA, and 1.76 kW. The source

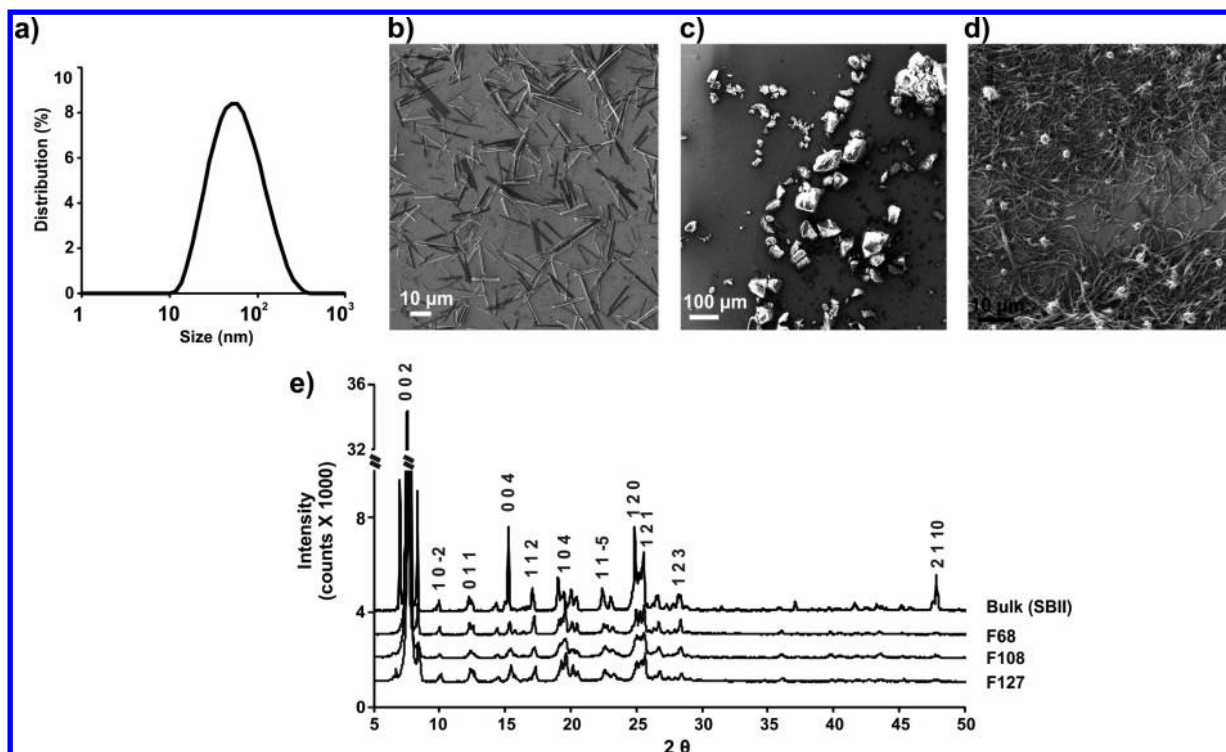


**Figure 2.** Pluronic effect on crystallizations. (a) Size distribution of Sudan blue II Pluronic micelles upon heating to 70 °C characterized by dynamic light scattering. SEM images of Sudan blue II microparticles crystallized in (b) Pluronic 10% (w/v) F108 solution, (c) commercial dyes (bulk crystals) and (d) microfibers formed from dissolving the dye (in an organic solvent) directly in water. (e) XRD patterns of bulk crystals and microcrystals of Sudan blue II formed with different Pluronic solutions.

of the diffractometer used, was a Cu K  $\alpha$  radiation at a 1.54 Å wavelength with a monochromator filter and analyzed in a  $\theta/2\theta$  mode at room temperature. The  $2\theta$  scan data were collected at a 0.030 interval, and the scan speed was 0.5 deg/min. The technique used for measuring intensities was the focusing beam method. Before X-ray diffraction measurement, crystals were centrifuged at 2000g for 5 min and resuspended in water, and this washing process was repeated twice to remove any free Pluronic from the surface of crystals.

### 3. RESULTS AND DISCUSSION

As shown in Figure 1a, anthraquinone dyes are tricyclic quinones which are fairly hydrophobic, and various commercially available derivatives with different substitutions were investigated. Anthraquinones were first dissolved in organic solvent and then were introduced slowly into an aqueous solution of Pluronic. As the organic solvent evaporated, the hydrophobic dyes formed nano or micro particles, with the aid of Pluronic. When the temperature of the solution was increased, the blue color of the anthraquinone Pluronic solution turned darker. Figure 1b shows 2  $\mu$ M Sudan blue II in 1% Pluronic F108 as it exhibited thermochromic behavior when the temperature was increased from 25 to 45 °C. Temperature-dependent absorption of Sudan blue II in Pluronic at different temperatures is shown in Figure 1c. At higher temperatures, two characteristic peaks of Sudan blue II dye were observed at 645 and 598 nm, which could possibly be attributed to  $\pi$ - $\pi^*$  and  $n$ - $\pi^*$  transitions, respectively.<sup>30</sup> At lower temperature, these two characteristic peaks disappeared and a longer wavelength peak appeared at 715 nm, with an isosbestic point at 665 nm. Bathochromic shifts can indicate the conversion to aggregates or crystals and are based on dye-dye interactions.<sup>30,31</sup> The absorption of other anthraquinones such as Sudan blue and D&C green at different temperatures is

shown in Figure 1, parts d and e, respectively. In Pluronic, both of these dyes also exhibited changes in absorbance with increasing temperatures. Thermochromism was not observed when anthraquinones were dissolved in another surfactant, Triton X-100 (Figure 1f) or in a DMPC liposome solution (Figure 1g). These alternative solubilization approaches did not impart thermochromic behavior to the dye, since those carriers themselves are not appropriately thermosensitive. The spectra of the dye in liposomes or Triton X-100 resembled that of the dye in Pluronic at elevated temperatures (where Pluronic micelles exist) suggesting the dye was similarly dispersed in those conditions. These spectra resemble that of the dye in solution in dimethylformamide (Supporting Information Figure S1). We previously demonstrated that hydrophobic dyes can be loaded into Pluronic micelles in noncrystalline form.<sup>32</sup> Reversibility is a key factor in practical thermochromic application and therefore the Sudan blue II Pluronic solution was subjected to heating and cooling cycles. As shown in Figure 1h, the thermochromism was fully reversible and after 10 heating and cooling cycles, no fatigue in the system was observed. The absorbance spectra of the 10 cycles are shown in Figure S2.

To better understand thermochromism, the size was first investigated using dynamic light scattering and scanning emission microscopy. At elevated temperature, the anthraquinone was dissolved in Pluronic micelles, with sizes around 50 nm (Figure 2a). At lower temperature, the solution became cloudy, indicating larger particles had formed, which was verified by scanning electron microscopy (SEM). As shown in Figure 2b, anthraquinones crystallized into microrods with a length of  $\sim$ 20  $\mu$ m using the reprecipitation method while the bulk materials (commercial dye as it was purchased) exhibited

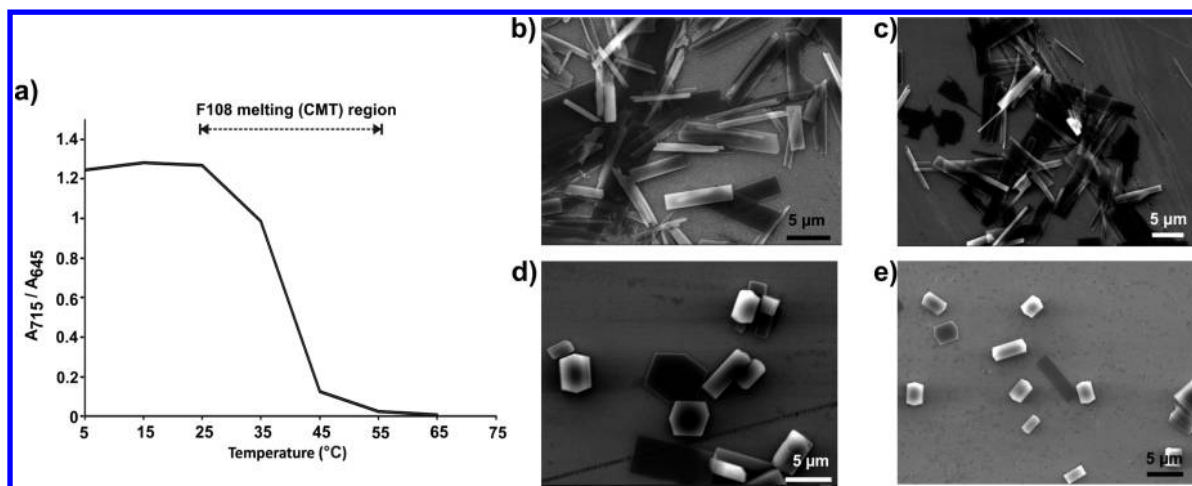


**Figure 3.** Temperature effect on crystallization in 1% Pluronic F108. (a) Thermochromic behavior of Sudan blue II. SEM images of microcrystals recrystallized at different temperatures (b) at 4 °C; (c) 25 °C; (d) 37 °C; and (e) 45 °C.

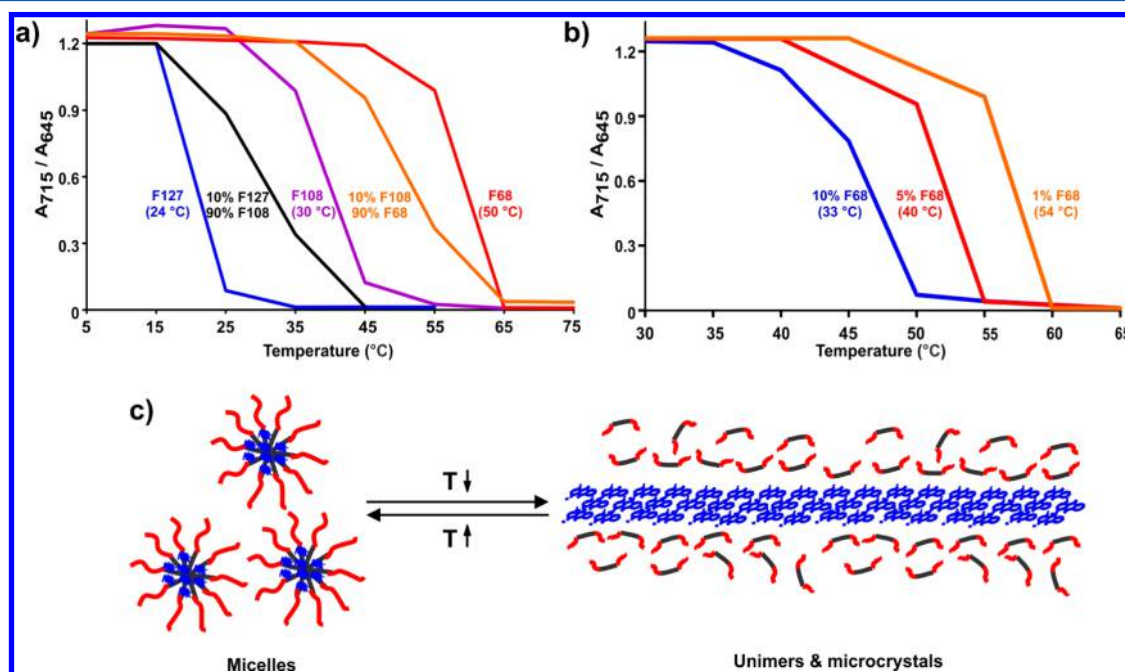


**Figure 4.** Thermochromism can be controlled by manipulating Pluronic micellization. (a) Thermochromism of Sudan blue II could be tuned by different types Pluronics (1% F127, 1% F108, and 1% F68 shown in the 1<sup>st</sup>, 3<sup>rd</sup>, and 5<sup>th</sup> lines, from left to right) or blended Pluronics (mixtures of 1% F127:F108 (vol/vol = 1:9) shown in the 2<sup>nd</sup> line and mixtures of 1% F108:F68 (vol/vol = 1:9) shown in the 4<sup>th</sup> line). (b) Thermochromism of Sudan blue II could be tuned by different concentrations of Pluronic (F68, 1%, 5%, and 10%). The numbers in parentheses indicate the reported CMT values of the corresponding Pluronic solutions. (c) Schematic illustration of micellization-dependent thermo-chromism.

irregular morphology (Figure 2c). Pluronic served not only to solubilize the anthraquinones at elevated temperatures, but also played a key role in dye crystallization. The dye was dissolved in organic solvent and was directly introduced into pure water without the presence of Pluronic. The morphology of the rods were fibrous in shape with longer lengths (Figure 2d), rather than microscale rods. The molecular interactions of Pluronic and dye likely inhibited dye–dye intermolecular interaction such as  $\pi$ – $\pi$  stacking, hence, the growth of crystals along the longitude direction was impaired. The structures of microcrystals (bulk crystals or the ones formed in Pluronic F127, F108, and F68 solutions) were investigated by X-ray diffraction (XRD) analysis (Figure 2e). The sharp peaks show that the microstructures are highly crystalline; no characteristic peaks of

Pluronic (found at 19° and 24°)<sup>33</sup> were observed, showing that Pluronic was not incorporated into the anthraquinone crystal structures. These bulk crystals and the ones formed in Pluronic solutions had the similar crystal habits, as shown in Table S1.

As the switching of anthraquinones between the micro- and nano- phase was temperature-dependent, the temperature effect in the presence of Pluronic (F108 used as an example) on the crystallization process was further investigated. As shown in Figure 1c, as the temperature increased from 5 to 55 °C, the absorption was thermally responsive, and the absorbance at 715 nm ( $A_{715}$ ) decreased sharply, whereas the absorbance at 645 nm ( $A_{645}$ ) increased sharply. As shown in Figure 3a, the ratio of the absorbance ( $A_{715}/A_{645}$ ) at the two wavelength dropped from 1.2 to 0, indicating that the dye migrated from

microcrystals to micelles between 35 and 45 °C. In this transition region, the characteristic absorption peaks of microcrystals at 715 nm disappeared gradually, whereas the characteristic peaks at 645 nm gradually appeared. Next, we studied the morphology of microcrystals formed below the CMT and in the transition region. The process of crystallization in Pluronic was conducted at different temperatures: 4, 25, 37, and 45 °C. SEM images show that at lower temperatures below the CMT (4 °C, Figure 3b and 25 °C, Figure 3c, below the CMT of 1% F108 that is 29.5 °C), microcrystals tended to be rod shape with a length of 8–10 μm whereas at higher temperatures (37 °C, Figure 3c and 45 °C, Figure 3d) the microcrystals formed with smaller size, being hexagonal or square shape with the length of around 2–3 μm. This can be explained with the reasoning that higher temperatures favored the dye solubilization process in the micelles, rather than the crystal formation process and higher temperatures impaired the growth of crystals in the longitudinal dimension.

Considering that the Pluronic micellization process is also temperature sensitive, we hypothesized that the micro- and nano- phase switching process was related to the micellization of Pluronic. Therefore, different types of Pluronic with different CMTs were employed to investigate thermochromism. As expected, the thermochromic transitions occurred at the temperatures of CMT of different Pluronics. Given that the CMT of 1% F127, F108, and F68 are 24 °C, 29.5 °C, and 50 °C, respectively, the thermochromic shifts of Sudan blue II crystals made and suspended in 1% F127, F108, and F68 occurred close to those CMTs (Figure 4a). The thermochromic transition temperature could be readily tuned by blending different Pluronics (Figure 4a) or different concentrations of Pluronic. Figure 4b shows an example of crystals made in 1%, 5%, and 10% F68 (with CMTs of 50 °C, 40 °C, 33 °C, respectively) and the onset of thermochromic transitions occurred close to those CMTs; comparison of CMTs and TTTs is shown in Table S2. Micellization-related thermochromism was based on the presence of micelles that existed only at elevated temperatures which served as carriers for hydrophobic anthraquinones. A conceptual representation of the thermochromism of anthraquinone in the presence of Pluronics is shown in Figure 4c. The formation of microcrystals or dye-loaded micelles are both driven by hydrophobic interactions. In the aqueous environment, in order to reduce surface energy, hydrophobic anthraquinones can interact either with other anthraquinones or with hydrophobic poly-(oxypropylene) (PPO) block of Pluronic. At elevated temperatures, Pluronic forms micelles with hydrophobic cores comprising primarily PPO blocks. Anthraquinone dyes tended to interact with PPO, rather than with other dye molecules probably because at elevated temperatures where micelles are present, interaction with PPO can minimize the surface energy. At lower temperature, Pluronic micelles dissociate into unimers, leaving no capacity for hydrophobic cargo to encapsulate in a hydrophobic phase-separated region and the dye tended to form microcrystals dominated by molecular interactions between the dyes. There should also exist interactions between dye and Pluronic as well that enabled microcrystals to be dispersed in aqueous solution, but interactions between dyes were favored probably because microcrystals gave minimized surface energy at lower temperatures.

## 4. CONCLUSIONS

In summary, we developed a tunable and fully reversible system to control the thermochromic behavior of anthraquinone dyes with the assistance of Pluronic block copolymers. The mechanism was based on temperature-dependent micro- and nano- phase switching, which unlike conventional thermochromism, can readily and precisely be tuned in a wide temperature range by the selection of different types, concentrations, or blends of Pluronics. Besides being able to manipulate micro- and nano- phase behaviors, these approaches could provide a convenient method to test CMTs of Pluronic by measuring TTTs. Such thermochromic materials might eventually be suitable for applications related to thermal sensors or temperature feedback systems.

## ■ ASSOCIATED CONTENT

### Supporting Information

The Supporting Information is available free of charge on the ACS Publications website at DOI: 10.1021/acs.langmuir.5b03095.

Figure S1, Absorbance spectra of Sudan blue II in dimethylformamide at various temperatures; Figure S2, Absorbance spectra of 10 heat/cool cycles of anthraquinone dye in Pluronic solution; Table S1, Crystal habit of microcrystals; Table S2, Comparison of CMTs and TTTs (PDF)

## ■ AUTHOR INFORMATION

### Corresponding Author

\*E-mail: jflovell@buffalo.edu (J.F.L.).

### Notes

The authors declare no competing financial interest.

## ■ ACKNOWLEDGMENTS

This work was made possible with support from the National Institutes of Health (DP5OD017898).

## ■ REFERENCES

- (1) Hu, J.; Zhang, G.; Liu, S. Enzyme-Responsive Polymeric Assemblies, Nanoparticles and Hydrogels. *Chem. Soc. Rev.* **2012**, *41* (18), 5933–5949.
- (2) Irie, M.; Lifka, T.; Kobatake, S.; Kato, N. Photochromism of 1,2-Bis(2-Methyl-5-Phenyl-3-Thienyl)perfluorocyclopentene in a Single-Crystalline Phase. *J. Am. Chem. Soc.* **2000**, *122* (20), 4871–4876.
- (3) Irie, M.; Sakemura, K.; Okinaka, M.; Uchida, K. Photochromism of Dithienylethenes with Electron-Donating Substituents. *J. Org. Chem.* **1995**, *60* (25), 8305–8309.
- (4) Qian, G.; Qi, J.; Davey, J. A.; Wright, J. S.; Wang, Z. Y. Family of Diazapentalene Chromophores and Narrow-Band-Gap Polymers: Synthesis, Halochromism, Halofluorism, and Visible–Near Infrared Photodetectivity. *Chem. Mater.* **2012**, *24* (12), 2364–2372.
- (5) CaroliáRezende, M. Interpretation of the Halochromism of Pyridiniophenoxide Dyes. *J. Chem. Soc., Faraday Trans.* **1992**, *88* (2), 201–204.
- (6) Yoshida, M.; Nakanishi, F.; Seki, T.; Sakamoto, K.; Sakurai, H. Two-Dimensional Piezochromism and Orientational Modulations in Polysilane Monolayer. *Macromolecules* **1997**, *30* (6), 1860–1862.
- (7) Kunzelman, J.; Kinami, M.; Crenshaw, B. R.; Protasiewicz, J. D.; Weder, C. Oligo(p-Phenylene Vinylene)s as a “New” Class of Piezochromic Fluorophores. *Adv. Mater.* **2008**, *20* (1), 119–122.
- (8) Walish, J. J.; Fan, Y.; Centrone, A.; Thomas, E. L. Controlling Thermochromism in a Photonic Block Copolymer Gel. *Macromol. Rapid Commun.* **2012**, *33* (18), 1504–1509.

- (9) Weissman, J. M.; Sunkara, H. B.; Tse, A. S.; Asher, S. A. Thermally Switchable Periodicities and Diffraction from Mesoscopically Ordered Materials. *Science* **1996**, *274* (5289), 959–960.
- (10) Matsubara, K.; Watanabe, M.; Takeoka, Y. A Thermally Adjustable Multicolor Photochromic Hydrogel. *Angew. Chem., Int. Ed.* **2007**, *46* (10), 1688–1692.
- (11) Ueno, K.; Matsubara, K.; Watanabe, M.; Takeoka, Y. An Electro- and Thermochromic Hydrogel as a Full-Color Indicator. *Adv. Mater.* **2007**, *19* (19), 2807–2812.
- (12) Reish, M. E.; Huff, G. S.; Lee, W.; Uddin, M. A.; Barker, A. J.; Gallaher, J. K.; Hodgkiss, J. M.; Woo, H. Y.; Gordon, K. C. Thermochromism, Franck–Condon Analysis and Interfacial Dynamics of a Donor–Acceptor Copolymer with a Low Band Gap. *Chem. Mater.* **2015**, *27* (8), 2770–2779.
- (13) Osborne, S. J.; Wellens, S.; Ward, C.; Felton, S.; Bowman, R. M.; Binnemans, K.; Swadźba-Kwaśny, M.; Gunaratne, H. Q. N.; Nockemann, P. Thermochromism and Switchable Paramagnetism of cobalt(III) in Thiocyanate Ionic Liquids. *Dalton Trans* **2015**, *44* (25), 11286–11289.
- (14) Guo, H.; Zhang, J.; Porter, D.; Peng, H.; Löwik, D. W. P. M.; Wang, Y.; Zhang, Z.; Chen, X.; Shao, Z. Ultrafast and Reversible Thermochromism of a Conjugated Polymer Material Based on the Assembly of Peptide Amphiphiles. *Chem. Sci.* **2014**, *5* (11), 4189–4195.
- (15) Sone, P. D. K.; Fukuda, P. D. Y. Inorganic Thermochromism. In *Inorganic Thermochromism; Inorganic Chemistry Concepts*; Springer: Berlin Heidelberg, 1987; pp 1–12.
- (16) Samat, A.; Lokshin, V. Thermochromism of Organic Compounds. In *Organic Photochromic and Thermochromic Compounds*; Springer: Berlin Heidelberg, 2002; pp 415–466.
- (17) Day, J. H. Thermochromism. *Chem. Rev.* **1963**, *63* (1), 65–80.
- (18) White, M. A.; LeBlanc, M. Thermochromism in Commercial Products. *J. Chem. Educ.* **1999**, *76* (9), 1201.
- (19) Chae, S. K.; Park, H.; Yoon, J.; Lee, C. H.; Ahn, D. J.; Kim, J.-M. Polydiacetylene Supramolecules in Electrospun Microfibers: Fabrication, Micropatterning, and Sensor Applications. *Adv. Mater.* **2007**, *19* (4), 521.
- (20) Yuan, Z.; Lee, C.-W.; Lee, S.-H. Reversible Thermochromism in Hydrogen-Bonded Polymers Containing Polydiacetylenes. *Angew. Chem.* **2004**, *116* (32), 4293–4296.
- (21) Wu, S.; Niu, L.; Shen, J.; Zhang, Q.; Bubeck, C. Aggregation-Induced Reversible Thermochromism of Novel Azo Chromophore-Functionalized Polydiacetylene Cylindrical Micelles. *Macromolecules* **2009**, *42* (1), 362–367.
- (22) Lu, Y.; Yang, Y.; Sellinger, A.; Lu, M.; Huang, J.; Fan, H.; Haddad, R.; Lopez, G.; Burns, A. R.; Sasaki, D. Y.; et al. Self-Assembly of Mesoscopically Ordered Chromatic Polydiacetylene/silica Nanocomposites. *Nature* **2001**, *410* (6831), 913–917.
- (23) Sato, O.; Tao, J.; Zhang, Y.-Z. Control of Magnetic Properties through External Stimuli. *Angew. Chem., Int. Ed.* **2007**, *46* (13), 2152–2187.
- (24) Morita, Y.; Suzuki, S.; Fukui, K.; Nakazawa, S.; Kitagawa, H.; Kishida, H.; Okamoto, H.; Naito, A.; Sekine, A.; Ohashi, Y.; et al. Thermochromism in an Organic Crystal Based on the Coexistence of  $\sigma$ - and  $\pi$ -Dimers. *Nat. Mater.* **2008**, *7* (1), 48–51.
- (25) Ohshima, A.; Momotake, A.; Arai, T. Photochromism, Thermochromism, and Solvatochromism of Naphthalene-Based Analogues of Salicylideneaniline in Solution. *J. Photochem. Photobiol., A* **2004**, *162* (2), 473–479.
- (26) Hadjoudis, E.; Mavridis, I. M. Photochromism and Thermochromism of Schiff Bases in the Solid State: Structural Aspects. *Chem. Soc. Rev.* **2004**, *33* (9), 579–588.
- (27) Wang, X.; Sandman, D. J.; Chen, S.; Gido, S. P. Thermochromic Polydiacetylene Micro- and Nanocrystals: An Unusual Size Effect in Electronic Spectra. *Macromolecules* **2008**, *41* (3), 773–778.
- (28) Piryatinski, A.; Ivanov, S. A.; Tretiak, S.; Klimov, V. I. Effect of Quantum and Dielectric Confinement on the Exciton-Exciton Interaction Energy in Type II Core/shell Semiconductor Nanocrystals. *Nano Lett.* **2007**, *7* (1), 108–115.
- (29) Rasenack, N.; Hartenhauer, H.; Müller, B. W. Microcrystals for Dissolution Rate Enhancement of Poorly Water-Soluble Drugs. *Int. J. Pharm.* **2003**, *254* (2), 137–145.
- (30) Yu, H.; Qi, L. Polymer-Assisted Crystallization and Optical Properties of Uniform Microrods of Organic Dye Sudan II. *Langmuir* **2009**, *25* (12), 6781–6786.
- (31) Balakrishnan, K.; Datar, A.; Oitker, R.; Chen, H.; Zuo, J.; Zang, L. Nanobelt Self-Assembly from an Organic N-Type Semiconductor: Propoxyethyl-PTCDI. *J. Am. Chem. Soc.* **2005**, *127* (30), 10496–10497.
- (32) Zhang, Y.; Jeon, M.; Rich, L. J.; Hong, H.; Geng, J.; Zhang, Y.; Shi, S.; Barnhart, T. E.; Alexandridis, P.; Huizinga, J. D.; et al. Non-Invasive Multimodal Functional Imaging of the Intestine with Frozen Micellar Naphthalocyanines. *Nat. Nanotechnol.* **2014**, *9* (8), 631–638.
- (33) Sruti, J.; Patra, C. N.; Swain, S. K.; Beg, S.; Palatasingh, H. R.; Dinda, S. C.; Rao, M. E. B. Improvement in Dissolution Rate of Cefuroxime Axetil by Using Poloxamer 188 and Neusilin US2. *Indian J. Pharm. Sci.* **2013**, *75* (1), 67–75.